AD-A036 318 NORTH AMERICAN AVIATION INC COLUMBUS OHIO COLUMBUS DIV F/G 17/1
HIGH POWER TRANSDUCERS.(U)
JUN 65 L RESNICK N140(70024)77479B
UNCLASSIFIED NA-64H-1257-5 NL

| OF |

AD
A036318

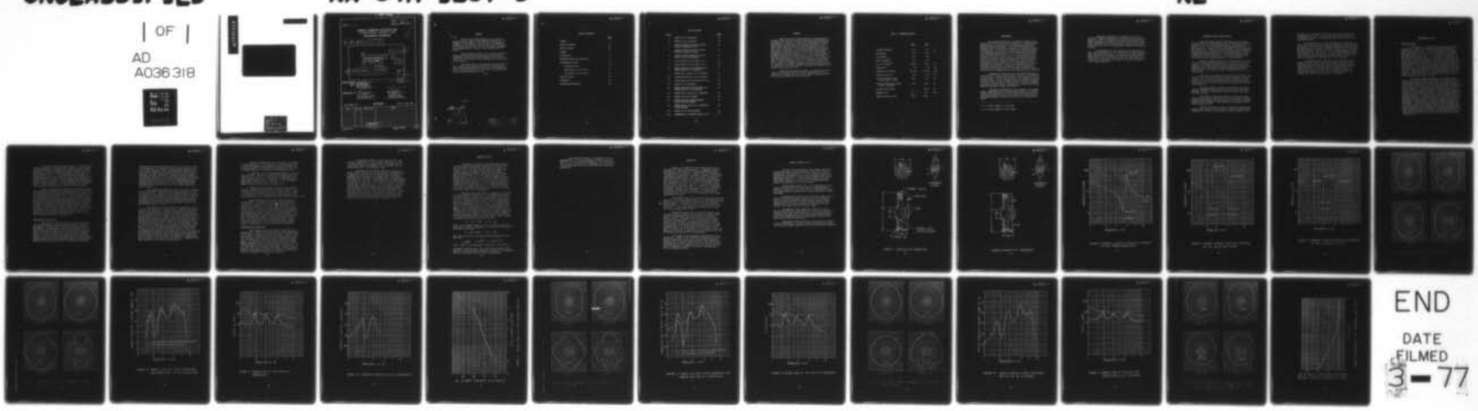

END
DATE
FILMED
3-77

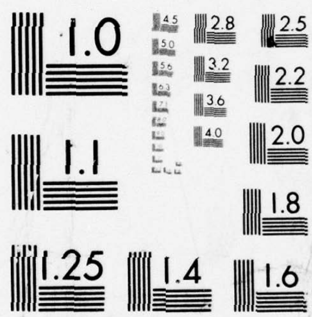
1.0
4.5
5.0
5.6
6.3
2.8
3.2
3.6
4.0
2.5
2.2
2.0
1.1
1.8
1.25
1.4
1.6

MOST ProJect - 4

4 June 1965

File No. ______ Report No. NA64H-1257-5

NORTH AMERICAN AVIATION, INC.

COLUMBUS DIVISION COLUMBUS 16, OHIO

ENGINEERING DEPARTMENT

(1)

(14) NA-64H-1257-5

(11) 4 Jun 65

(6) HIGH POWER TRANSDUCERS.

(12) 39p.

(9) FINAL REPORT,

(15) N140(70024)77479B

PREPARED BY Leon Resnick
(10) Leon Resnick
Project Engineer
Marine Acoustics

APPROVED BY W. J. Toulis
W. J. Toulis
Sr. Project Engineer
Marine Acoustics

R. Holden
R. Holden
Program Manager
ASW Marine Systems

No. of Pages 34 REVISIONS Date 4 June 1965

DATE	REV. BY	PAGES AFFECTED	REMARKS

E D H 337 (REVISED 9-12-55)

401941

PREFACE

The Contract N140(70024)77479B entitled "High Power Transducers" was issued to North American Aviation, Inc. at Columbus, Ohio by USNUSL as the first part of a program to evaluate a 15-foot acoustic Luneberg lens. The first phase is to design, fabricate and test two piezoceramic transducers to radiate 60-100 kw of acoustic power in water at 2.6 to 3.0 kc.

North American Aviation, Inc. at Columbus has manufactured the two transducers and evaluated them at NRL's Calibration Station on Lake Seneca during the week of 19-23 April 1965. The results of this investigation are incorporated in this report.

The second phase of the program will involve the 15-foot compliant tube Luneberg lens with five transducers in order to demonstrate performance and source levels comparable to the latest submarine sonars. This lens is already in existence and would be supplied by ONR.

TABLE OF CONTENTS

LIST OF FIGURES

SUMMARY

Since the acoustic output depends on both the amount of the piezoceramic material and also the effective electromechanical coupling factor, the basic design of the flextensional transducer was modified to accommodate a piezoceramic stack which is considerably longer than the diaphragm. The design requires only a simple oil fill and thus the transducer is usable at any depth at sea. Table I summarizes the pertinent characteristics of the two transducers as recorded at NRL-Lake Seneca and at NAA-Columbus. Cavitation limited the radiated power to 30 kw at 500 ft depth, but extrapolation of the data indicates that a power of 85 kw would have been attained with 4 KV rms in the absence of cavitation. Although the mechanical Q_m of 6 at the 2.8 kc resonance is somewhat high, the useful bandwidth of the F2-1 transducer is really much wider. Within the frequency band from 2.5 kc to more than 4.0 kc, the transducer can radiate a minimum of 30 kw when driven with 4 KV, or a minimum of 45 kw with 5 KV which represents the maximum usable voltage at very low duty cycles.

Further source level measurements are suggested to demonstrate the full power capability of the transducers, as well as suitable pulse lengths and duty cycles. Mutual coupling tests and tests with the 15-foot lens are also planned.

TABLE I. TRANSDUCER SUMMARY

	F2-1	F2-2	
Resonant Frequency	2.8	2.8	kc
Q_m (Bridge)	6.1	6.0	
Q_e (Bridge)	1.0	1.2	
$Q_{eff} = (Q_e Q_m)^{1/2}$	2.5	2.7	
$k_e = (1 + Q_e Q_m)^{-1/2}$	37.6	35.0	%
Capacitance	.70	.70	mfd.
Impedance at Resonance	87 -j87	68 -j83	ohms
Directivity Index	3.3	3.8	db
Source level/volt (omni) (Re: 1 mbar at 1 yd)	48.7	50.1	db
Receiving Sensitivity (omni) (Re: 1 volt/mbar)	-77.8	-76.4	db
Acoustic Power Output	--	25-30	kw
Weight in Air	75	85	lbs
Depth Limitation at Sea	None	None	

INTRODUCTION

The principle objective of the subject contract was to demonstrate that the flextensional transducer can combine suitable electroacoustic characteristics with compactness and extremely high power handling capability. Previous investigations have indicated that the flextensional transducer is especially suitable for the purpose. Its unusual structure permits the piezoceramic to be highly prestressed without degrading appreciably the effective electromechanical coupling factor. This is attained with a prestress spring which does not block the piezoceramic material because the stiffness of the spring is counterbalanced by inertance at the desired frequency of operation.[1] More specifically, the prestress spring is provided by the mechanically resonant diaphragms of the transducer which are highly flexible at the desired operating frequency. Thus the key advantage of the flextensional transducer over conventional designs of comparable structure is the replacement of the prestress spring that blocks with one which is highly flexible at the preferred band of operation.

Although the prestress in the piezoceramic stack may be very large, the corresponding mechanical stresses in the diaphragms are not likely to be excessive in terms of the fatigue life of the diaphragm walls. This is primarily because the diaphragm dimensions have to be thick in order to attain the desired resonant frequency and also because a large radiating surface is desired to minimize cavitation in shallow water. Alternatively, the walls must also be thick for operation at great ocean depths.[2]

The thermal dissipation is also enhanced by the specific design incorporated with the flextensional transducer. The piezoceramic stack consists of a series of short disks interlaced with thin copper disks which serve as electrodes and conduct the heat generated internally in the stack to the oil fill surrounding the stack.

- -

[1] W. J. Toulis, JASA 35, 74-80 (1963)

[2] W. J. Toulis, JASA 37, 250-256 (1965)

Although the combination of high power and a small transducer is readily susceptible to cavitation at shallow depths, there are a number of techniques by which cavitation may be minimized. Deaeration and control of the viscosity of the enveloping liquid represent the two simplest methods. Pressurization of the same liquid can also be used provided the enclosure is transparent to sound.

In designing the subject transducer for optimization of power, the above factors were in evidence and taken into consideration. The transducer design is an outgrowth of a similar experimental unit that was investigated at NAA; both the frequency and power output of the latter were lower with the result that the design had to be modified to some extent to fulfill the objectives of the subject transducer.

TRANSDUCER DESIGN AND FABRICATION

The basic design of the two transducers (to be referred to here as F2-1 and F2-2) originated from an experimental transducer (F1 series) that was investigated previously. The sketches in Figures 1 and 2 are representative of the dimensions of the F2-1 and F2-2 transducers. These differ only externally: thinner diaphragms and cylinder walls. Compared to the F1 version these are shorter in length to attain a greater stiffness from the PZT stack but larger in diameter to minimize cavitation. The greater stiffness in the stack was intended to minimize the effect of mass-loading of the end sections on the resonance frequency of the transducer.

The F2-2 transducer consists of a steel shell 17.75 inches long with a maximum diaphragm diameter of 7.5 inches and a 14 inch long by 3 inch diameter piezoceramic stack centered in the shell. (Figure 1). The shell has twelve diaphragms and two chimney pieces. The diaphragms are the result of twelve lengthwise slots in the bulbous section. The chimney sections are cylindrical having a 4.6 inch diameter.

The ends of the transducer are closed off with plugs. One plug is held in place with tapered pins while the other is threaded in place. The threaded end is used to apply the prestress to the ceramic stack. A floating steel disc is used between the threaded plug and the stack to take out the torsional load during application of the prestress.

The whole assembly is sealed by stretching a rubber boot over the diaphragm section and using "O" rings at all other shell openings. With this configuration no other containers are required for tests in water.

The internal volume of the transducer is filled with de-aereated silicone fluid. The fluid acts as a dielectric to eliminate arcing between the stack and shell and also as an acoustic pressure release for the diaphragms. The viscosity of the silicone fluid is 100 centistokes in F2-2.

The F2-1 transducer is similar to F2-2 with the same piezoceramic stack, however, the shell has been modified by thinning the diaphragms and portions of the chimneys as shown in Figure 2. The

diaphragm walls which were .69" are now .50" and the chimneys were thinned from .50" to .25". Also the silicone fluid was changed to 10 centistoke viscosity. These modifications and their effects will be discussed later.

The transducer shells were fabricated in one piece from a solid steel billet to keep the structure homogeneous. Rough machining of the shells was done with the material annealed. After the material was heat treated to an ultimate strength of 180-200,000 psi, the shell was finish machined. All the other pieces were machined in the high heat treated state. The tolerances observed during machining kept the stack alignment caps parallel and concentric within .001 inch. Since steel is susceptible to corrosion, all external parts of the transducer were plated with a .0004 inch thick layer of cadmium.

Fabrication of the piezoceramic stack consisted of bonding together the PZT-4 disks, and alternating them with copper disks. The adhesive was applied to the mating surfaces, then the ceramic disks were placed in a jig with a copper disk between the PZT disks and the PZT-4 faces of the same polarity facing each other. In addition, fused silica and steel disks are added to the ends to electrically insulate the stack from the shell and provide added strength where high loading can occur during handling.

EXPERIMENTAL PROGRAM

Preliminary Tests

In addition to the measurements at Lake Seneca and NAA's earthwall pool, the two transducers were examined mechanically, dynamically and electrically. Mechanical testing of the transducers consisted of a static test of the F2-2 shell to determine the spring constant and stresses of the structure. Before testing the shell, strain gages were mounted longitudinally along two lines 180 degrees apart at the diaphragm center, at both diaphragm root points, and on both chimneys. The shell was then mounted in a fixture, using shims where necessary to insure that only axial loads could be transmitted to the shell. Deflections were measured with potentiometers, accurate to $\pm$ .0005 inches, mounted at one end of the transducer. Loads up to 80,000 pounds were applied to the shell with strain gage and potentiometer readings recorded at 5,000 pound intervals. From these readings, it was deduced that the F2-2 structure has a spring constant of 5×10^6 pounds/inch when the force is applied axially at the ends. The maximum stress to load ratio was found to be 0.8 psi per pound of force.

The relative motional amplitudes and vibrational mode shapes of the transducers were determined by exciting the PZT stack in the transducer and recording the output from a unidirectional accelerometer mounted to it. Since dynamic excitation was limited to that due from the PZT stack, it was only possible to examine modes that are inherent to such vibrational excitation. These were primarily extensional, but bending and torsional vibrations can be induced also as a result of asymmetry. Actually only the amplitude and phase of the accelerometer signal were recorded for a number of points on the shell. The phase of the signal was determined from a Lissajous figure on an oscilloscope with the node being at the point the signal reversed its phase. With this set-up and the measurements along a circumference, the amount of chimney bending could be determined. As the transducer was originally built, bending was very much in evidence, but changing the pins from straight to taper at one end and to a large torquing screw at the other brought the bending amplitudes in air down to 10% of the peak diaphragm motion. Since a unidirectional accelerometer was used, twisting modes of the shell could not be observed but it is suspected that they may be significant especially in water where the pulsating mode is damped by radiation.

The principal electrical measurements in air involved the frequency response at constant current. Figure 3 is for the piezoelectric stack alone, and Figure 4 is the F2-2 transducer without the oil fill. The electromechanical coupling coefficient of the stack alone is 56% at 4.0 - 4.8 kc whereas it drops to 35% for the F2-2 transducer at 2.3 kc. The latter represents the combined resonance frequency of the housing and stack. The coupling at 35% is not as high as anticipated primarily because the resonance frequency at 2.3 kc is too low to permit lengthening of the diaphragm slots as conceived originally, for improved coupling. The resonance at 4.7 - 5.1 kc in Figure 4 essentially represents the "stretch" rather than the flexural mode of vibration in the diaphragm.

Figure 5 represents the frequency response in air of the F2-2 transducer when filled with silicone fluid 200/100 centistokes. The response differs quite markedly from that shown in Figure 4 without the oil fill. The resonance at 2.3 kc has disappeared but it has been replaced by one or two at 1.6 - 2.0 kc and another at 2.9 kc. The reason for this breakup is not clear. In fact, additional measurements with the transducer partially filled with oil suggests that the 2.9 kc resonance might have migrated downward from the 5.0 kc region. Measurements with liquids having different compressibilities and densities might shed some light but it has not been convenient to investigate this aspect at this time. However, there are indications that these irregular resonances would disappear if the length of the transducer could be shortened; that is, such behavior was never noticeable until the chimney concept was introduced for high power output considerations.

Measurements at Lake Seneca

Measurements at NRL's Calibration Station on Lake Seneca involved polar patterns, frequency response data and high power evaluation at different depths. The polar patterns for the F2-2 (see Figure 1) are completely circular in the equatorial or XY plane but not in the YZ plane which contains the ends. The latter patterns are shown in Figures 6 and 7 at frequencies ranging between 1.7 and 4.8 kc. These polar patterns are not circular but "appear" to radiate from the ends rather than from the diaphragm surface. This is because the diaphragms vibrate in unison along the equatorial belt; the far field radiation from each element on the belt tends to be in phase with other contributions in directions

towards the ends but considerably out of phase in directions close to the equatorial XY plane; the diameter of the transducer relative to the wavelength of sound is an approximate measure of the lack of phase conherence in the equatorial plane. From this interpretation, the lower frequency polar patterns should be rounder than those at higher frequencies. Actually, the unusual length of the transducer compared to its diameter distorts this simple picture so that the polar pattern tends to be more omnidirectional at frequencies above 2.5 kc up to about 4.0 kc. Furthermore, properly positioned refractive material can be used to remold these polar patterns to yield nearly omnidirectional as well as highly directional patterns.

The transmitting response in Figure 8 of the F2-2 indicates that there are three frequencies where resonance appears to occur: 1.7, 2.8 and 4.8 kc. The one at 4.8 kc represents the stretch mode of vibration in the diaphragm with appreciable radiation coming also from the ends of the transducer. The resonance at 2.8 kc is due to the flexural motion of the diaphragms in conjunction with the mass provided by the end sections; that is, the resonance frequency of the diaphragm is about 4.0 kc but the undue amount of mass in the end sections lowers it to 2.8 kc.

The resonance at 1.7 kc in Figure 8 is unexpected in the sense that it seems to be associated with a parasitic type of motion which was not anticipated. Although a bending type of motion was indicated through probing, a torsional vibration is being suspected as the partial cause of the resonance at 1.7 kc and the adjacent hole in the response at 2.1 kc. Further, corroborative evidence can be deduced from the bridge measurements shown in Figure 9 by calculating the resultant frequency response in terms of the electrical power input; the equivalent electrical input level is also shown in Figure 8. Aside from a correction of 3-4 db due to the directivity pattern, the two curves coincide almost exactly except at frequencies below 2.5 kc. At 1.7 kc for example, the acoustic level is down almost 10 db when corrected for the directivity index (DI). With such a low efficiency, the mechanical resonance must be due to a motion which is nonradiative and highly viscous. Thus such a descriptive behavior fits the torsional much more than the bending mode and especially since the polar patterns do not show any evidence of a bending mode; that is, bending of the transducer would show up as asymmetry in the polar patterns in the XY plane of the transducer.

The F2-2 transducer was run as a receiver; its response is shown in Figure 10. The sharp null in both the transmitting and receiving response is not uncommon and is usually caused by a change in radiation mode between two resonances. In this case the lossy mode at 1.8 kc shifts to a radiating mode at 2.8 kc.

In addition to the calibration measurements, high power tests were made. Basically they consisted of pulsing the tuned transducer with a 175 kw Ling amplifier while measuring the current, voltage and phase at the transducer. A calibrated hydrophone spaced 5 meters from the transducer on a boom arrangement measured the sound field along the Y axis.
NOTE: The other data was taken along the Z axis.

A number of runs were made at depths of 260, 360 and 500 feet. Cavitation was present at all depths, however, input power was measured accurately only at the 500 foot depth. Figure 11 shows the sound pressure field varies linearly in the absence of cavitation with the voltage applied to the transducer. Cavitation limited the power to 25-30 kw with 2850 volts at the 500-ft depth.

The second transducer, the F2-1, was calibrated also at Lake Seneca. It differed from F2-2 in having a diaphragm thickness of 0.50 instead of 0.69 and a cylindrical wall thickness of 0.25 instead of 0.50 inches. Figure 12 shows a series of polar patterns which do not differ appreciably from those in Figures 6 and 7 for the F2-2. The frequency response in Figure 13 is also similar to that for F2-2 but with a lower mechanical Q and somewhat more uniform response at frequencies above 2.5 kc; the correlation between the sound pressure field and that deduced from the bridge data in Figure 14 is also more uniformly consistent. Thus the F2-1 appears to have somewhat better electroacoustic characteristics than the more massive F2-2. However, it was not convenient to drive the F2-1 to high power output, though it should behave not unlike the F2-2 in this respect.

Measurements at NAA-Columbus

Both transducers were calibrated at NAA-Columbus with results which in general are fairly consistent with those observed at Lake Seneca. However, there was one specific situation where the two sets of measurements showed considerable diversity. The polar patterns in the YZ plane for the F2-2, and shown in Figure 15, were considerably rounder than those in Figure 6 from Lake Seneca. The measurements at NAA's earthwall pool were recorded before Lake Seneca tests as well as after and using both pulsed and CW techniques without any apparent change in the outcome. On the other hand, the discrepancy with the F2-1 transducer was not as great. Thus with this limited information, it is not certain whether the discrepancies arose due to the method of calibration or due to the method of supporting the transducer.

The frequency response in terms of source level and electrical impedance were also recorded at NAA-Columbus. These are shown respectively in Figures 16 and 17 and agree fairly closely with those at Lake Seneca in view of the fact that the NAA earthwall pool is not especially large.

An attempt was also made to determine the influence of a small conical reflector for use with one of the transducers as an appropriate prime feed for the lens and also as a means to minimize mutual coupling between adjacent feeds. The conical reflector was of the right circular type with a 10" diameter and with steel walls 0.50 thick. Figures 18a and b show polar patterns at 2.0 and 3.0 kc with the conical reflector in place; the front-to-back ratio is only 5 db at 3.0 kc and 2 db at 2.0 kc; the front-to-side ratio is better at 6 and 12 db, respectively. When cell-tite is placed behind the conical reflector, Figures 18c and d, the front-to-back ratio is improved to 9 and 7 db respectively while the front-to-side ratio is essentially unaltered. Although these are promising results, a much greater front-to-side ratio is anticipated when the conical reflector is overfilled with a low-velocity liquid; thus the mutual coupling with other transducers in proximity should be greatly reduced as a result.

ANALYSIS OF DATA

The design of the F2-series of transducers resulted originally from the design and investigation of the F1-series which had chimney sections even longer than those shown in Figures 1 and 2. The resultant electroacoustic response was similar in spite of attempts to alter them by thinning out the diaphragms of the F2-1 relative to those of the F2-2. Based on this evidence, the shorter chimney sections of the F2-series relative to those of the F1-series suggests that the chimney sections are not sufficiently short as yet if the diaphragms rather than the massive end sections are to control the preferred resonant frequency. It is anticipated that shorter chimney sections and some modifications in diaphragm dimensions would result in a larger electromechanical coupling factor and also a lower mechanical Q without serious sacrifice in the maximum acoustic power that can be radiated.

The source level measurements in Figure 11 for the F2-2 show that the acoustic output is limited severely by cavitation at 500-foot depths. This situation is unexpected only in terms of the well known assumption of 1/3 watt/cm^2 near the surface of the water. Actually, the latter generalization is applicable to transducers with dimensions which are relatively large when compared to the wavelength of sound in water. For a smaller transducer, the near-field pressure can be much greater than might be expected from the extrapolation of far-field measurements. For example, a pulsating sphere radiates an acoustic power equal to V^2R_r where R_r is the resistive component of the radiation load and v is the velocity of vibration of the sphere surface. However, far-field measurements cannot tell anything about v and R_r except that the combination leads to an acoustic power of v^2R_r. On the other hand, the radiation load on the sphere is

$$Z_r = R_r + j\omega M_r = R_r\ (1 + jQ)$$

where ω is the angular frequency, M_r is the radiation mass on the sphere and $Q = \omega M_r/R_r$. Consequently, the pressure on the sphere is not simply vR_r but rather

$$p = v\ (R_r + j\omega M_r) = v\ R_r\ (1 + jQ)$$

and in terms of the far field pressure (p_a) extrapolated to the near field

$$|p/p_a| = (1 + Q^2)^{1/2} = \left[1 + (ka)^{-2}\right]^{1/2}$$

where $k = \frac{2\pi}{\lambda}$, λ is the wavelength of sound and a the radius of the sphere. The above ratio, of the near field to the far field pressure, is shown plotted in Figure 19 as a measure of the degradation of the cavitation limit as defined conventionally.

Since the F2-2 transducer is estimated to have an equivalent ka = 0.8 with an equivalent surface area of about 80-100 in^2, then the predicted degradation in the cavitation limit is 4 db. Consequently, the measured output of 25-30 kw is not inconsistent with the 75 kw expected from conventional assumptions.

CONCLUSIONS

Table I is a summary of the performance data of the F2-1 and F2-2 flextensional transducers. In general, these are consistent with the objectives of Contract N140(70024)77479B. The transducers were designed to handle 60-100 kw at mechanical resonance and the measurements in Figure 11 support this objective even though the actual power output was limited by cavitation to 25-30 kw at 500-foot depths. More specifically, the radiated acoustic pressure is known to be linear with the applied voltage and, consequently, the output should be 85 kw with 4000 volts and 132 kw with 5000 volts. The latter is the limiting voltage for the onset of depoling in PZT-4 and, therefore, it should be approached only at low duty cycles in order to avoid undue heating effects. However, this performance is attainable at most any depth at sea inasmuch as the properties of the pressure-release material, silicone fluid in this instance, do not change appreciably with depth.

The mechanical Q_m of 6 is somewhat high but the electrical Q_e of one is low so the effective Q_{eff} is 2.5. The latter deduction appears to be justified especially by the frequency response of the F2-1 in Figure 13. The latter indicates that the useful band extends from 2.5 kc to more than 5 kc. Even at the lowest output level at 3.4 kc, the power output can be as high as 40 kw with the limiting voltage of 5000 volts.

Although efficiency was not measured directly, it can be deduced from the comparison of the source level measurements with the corresponding power input equivalents as shown in Figures 9 and 13. The source level curves are higher because of a directive gain of about 2 to 4 db, depending on the polar pattern at each frequency. On deducting the correction due to directive gain, the resultant difference between the two curves is of the order of one db at frequencies above 2.5 kc. At lower frequencies and 1.7 kc in particular, the difference is of the order of 10 db so that the efficiency is of the order of 10%. The latter is attributed to a parasitic torsional vibration which cannot radiate in the manner of the pulsating mode.

As a result of the experimental evaluation of the two transducers, it appears that an improved electromechanical factor and wider mechanical resonance can be attained by reducing the lengths of the cylindrical chimney sections. More specifically, the large mass in these sections has distorted the initial design objectives wherein the diaphragm controls, principally, the frequency of mechanical resonance. As a result, the diaphragm is not now configured optimally.

RESEARCH RECOMMENDATIONS

In view of the acoustic power being limited to 25-30 kw by cavitation, power output capabilities beyond 100 kw should be verified with the F2 transducers in waters deeper than 500 feet. Alternatively improvements of 5-10 in the cavitation limit can be expected with deaerated transformer oil and somewhat more with the more viscous castor oil. A third approach involves a thin-wall pressurized container but the design of the acoustically transparent shell represents an added complication.

The essentially simple design of the flextensional transducer, with only an oil fill as the pressure-release material, permits it to operate at any depth at sea. An experimental evaluation should show that the power output remains practically unaltered with depth.

Approximately one-third of the transducer length should be eliminated from the cylindrical portions of the F2-2 transducer. Such a structural modification should yield an improved electromechanical coupling factor, a broader frequency response, lower mechanical Q_m at the pulsating mechanical resonance of the diaphragms, and a nearly comparable acoustic output.

The emphasis of thin (0.200 inch thick) disks in the piezoceramic stack with copper electrodes, to serve as cooling fins as well, should permit the dissipation of a large amount of heat from within the piezoceramic stack under high duty cycle operation. A test of the temperature rise vs. average power will reveal the usable duty cycle at any power level.

Measurements with the ONR 15-foot lens should be initiated in order to demonstrate a practical ability to control both cavitation and mutual coupling suppression under high power output conditions.

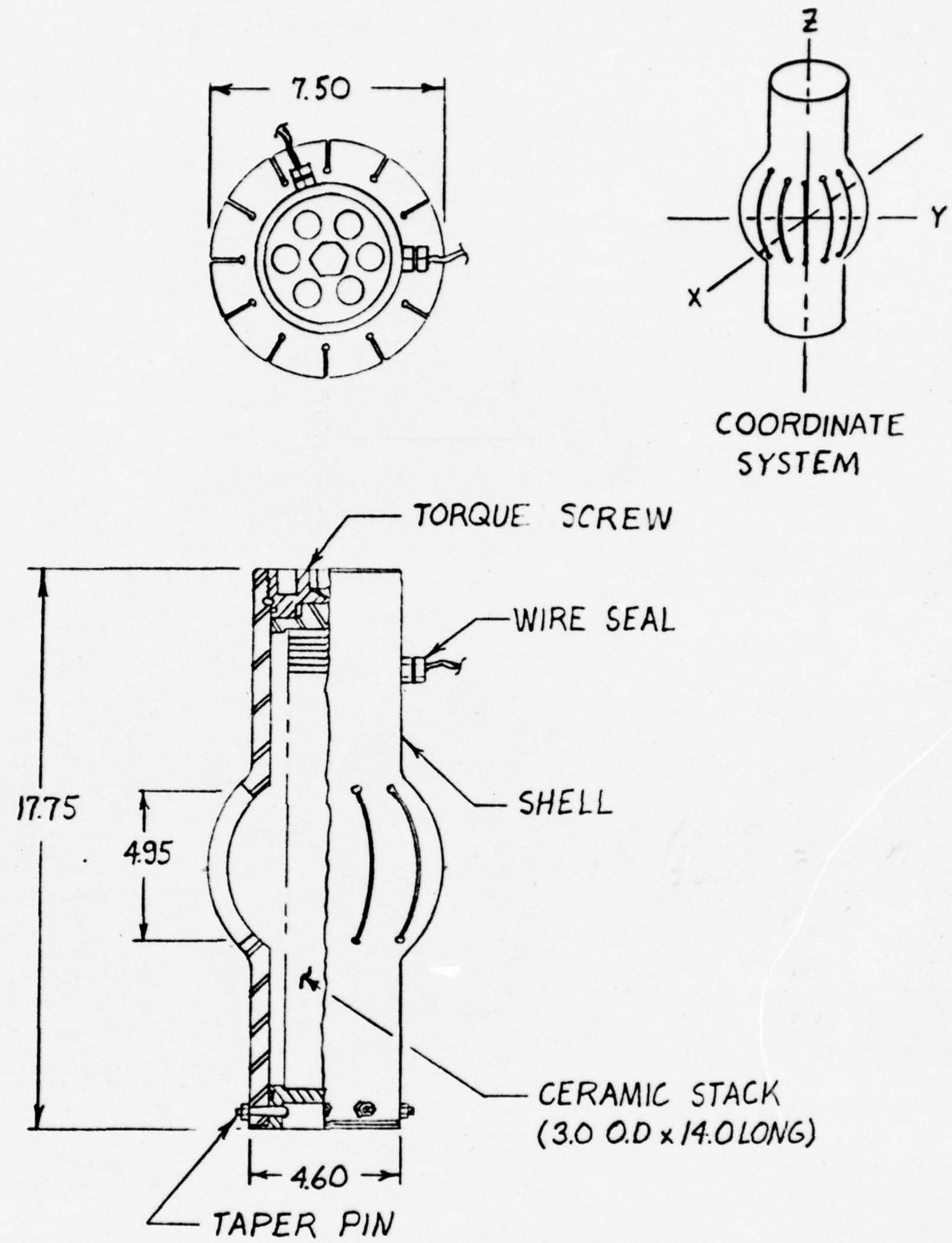

FIGURE 1. SKETCH OF F2-2 TRANSDUCER

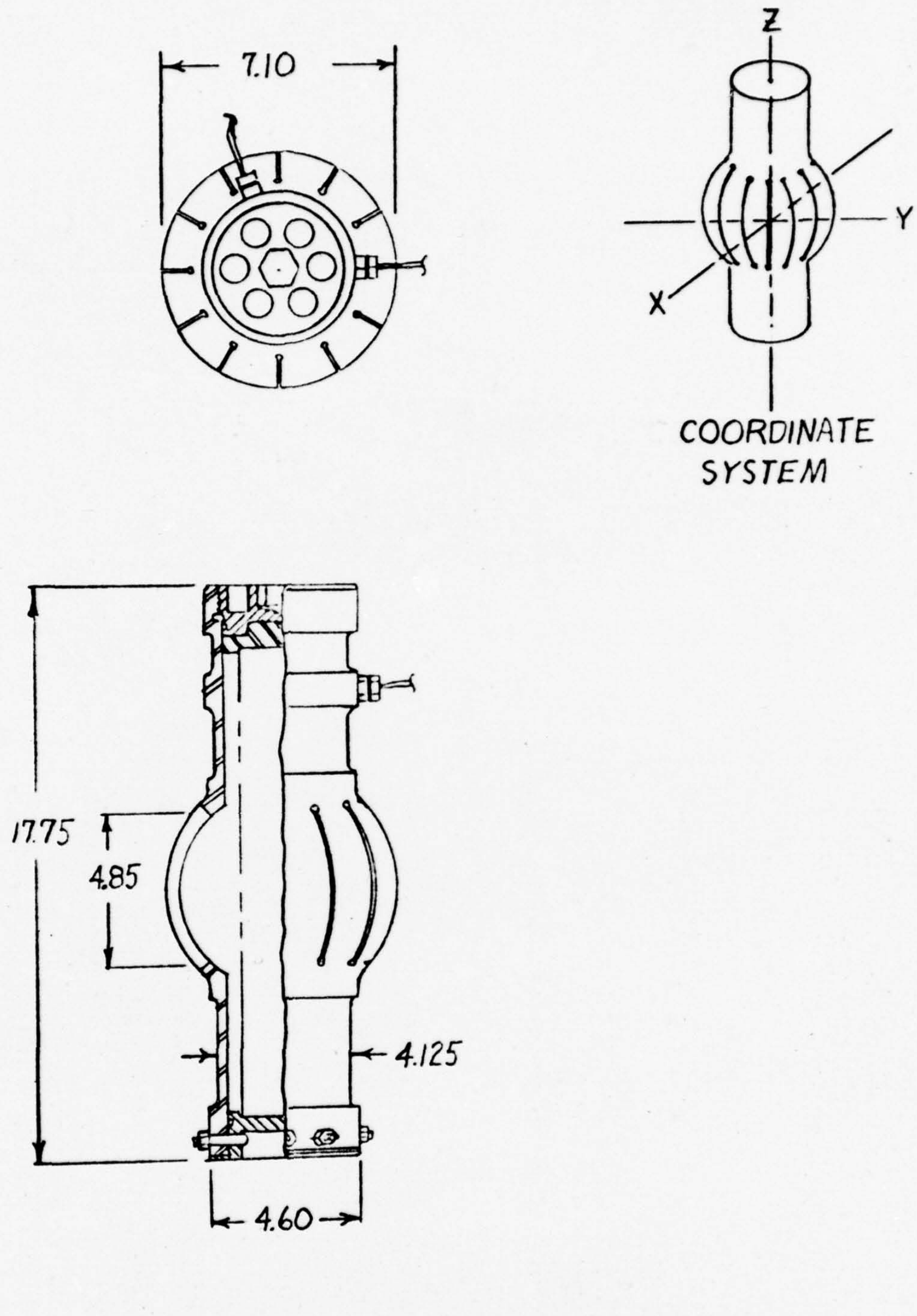

FIGURE 2. SKETCH OF F2-1 TRANSDUCER

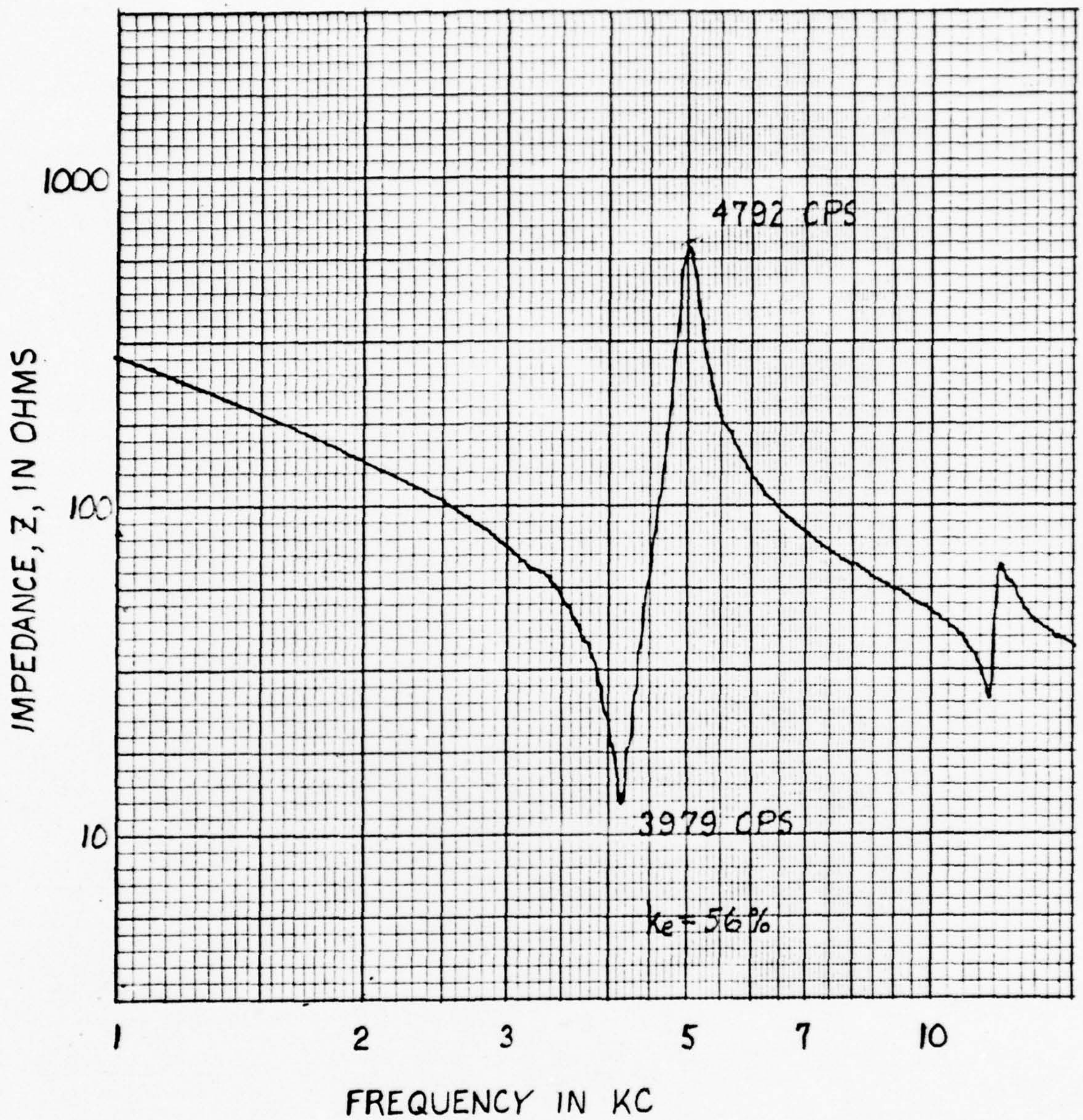

FIGURE 3. CONSTANT-CURRENT FREQUENCY RESPONSE OF F2-2 PIEZOCERAMIC STACK

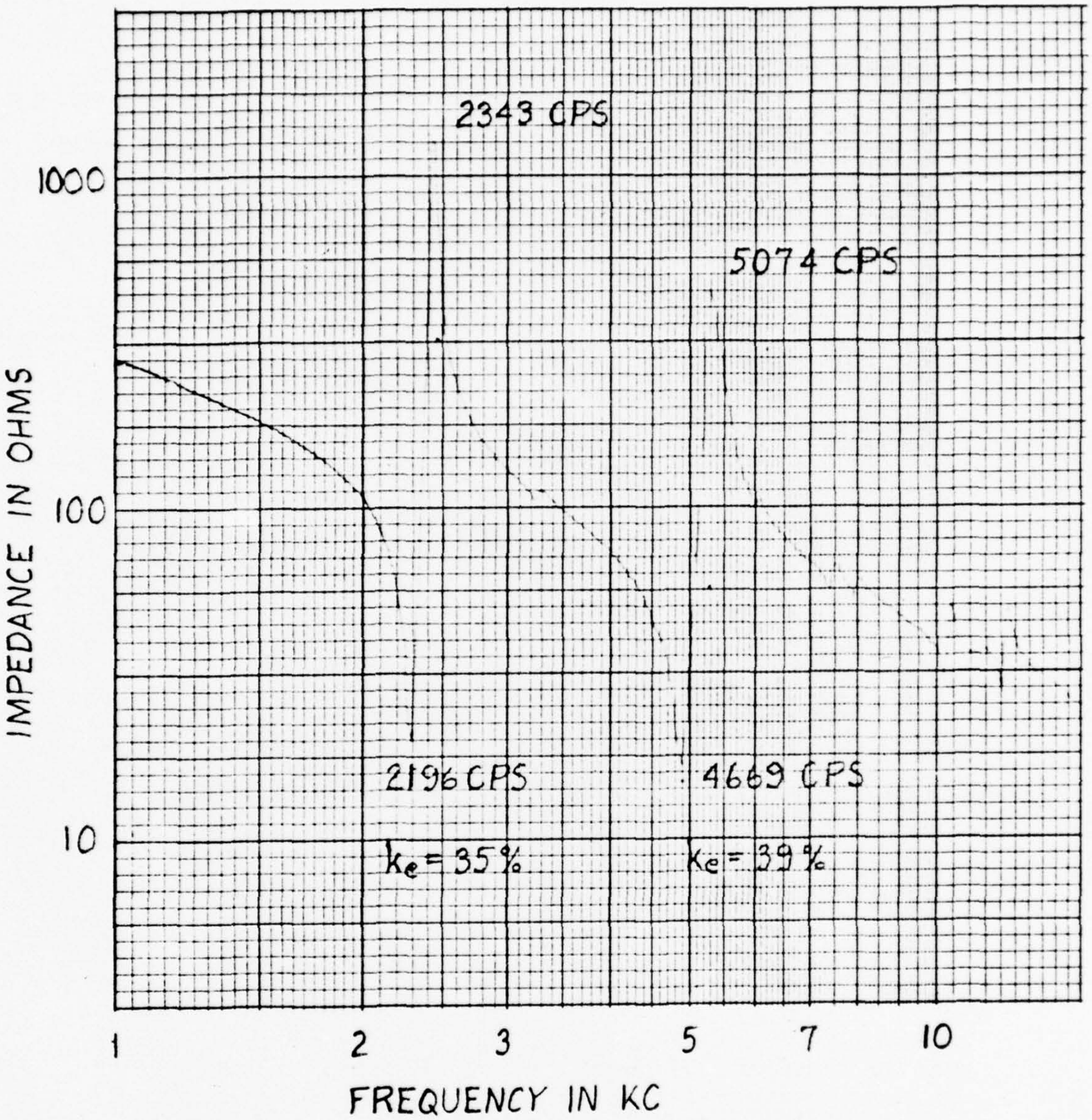

FIGURE 4. CONSTANT-CURRENT FREQUENCY RESPONSE OF F2-2 IN AIR (AIR FILLED)

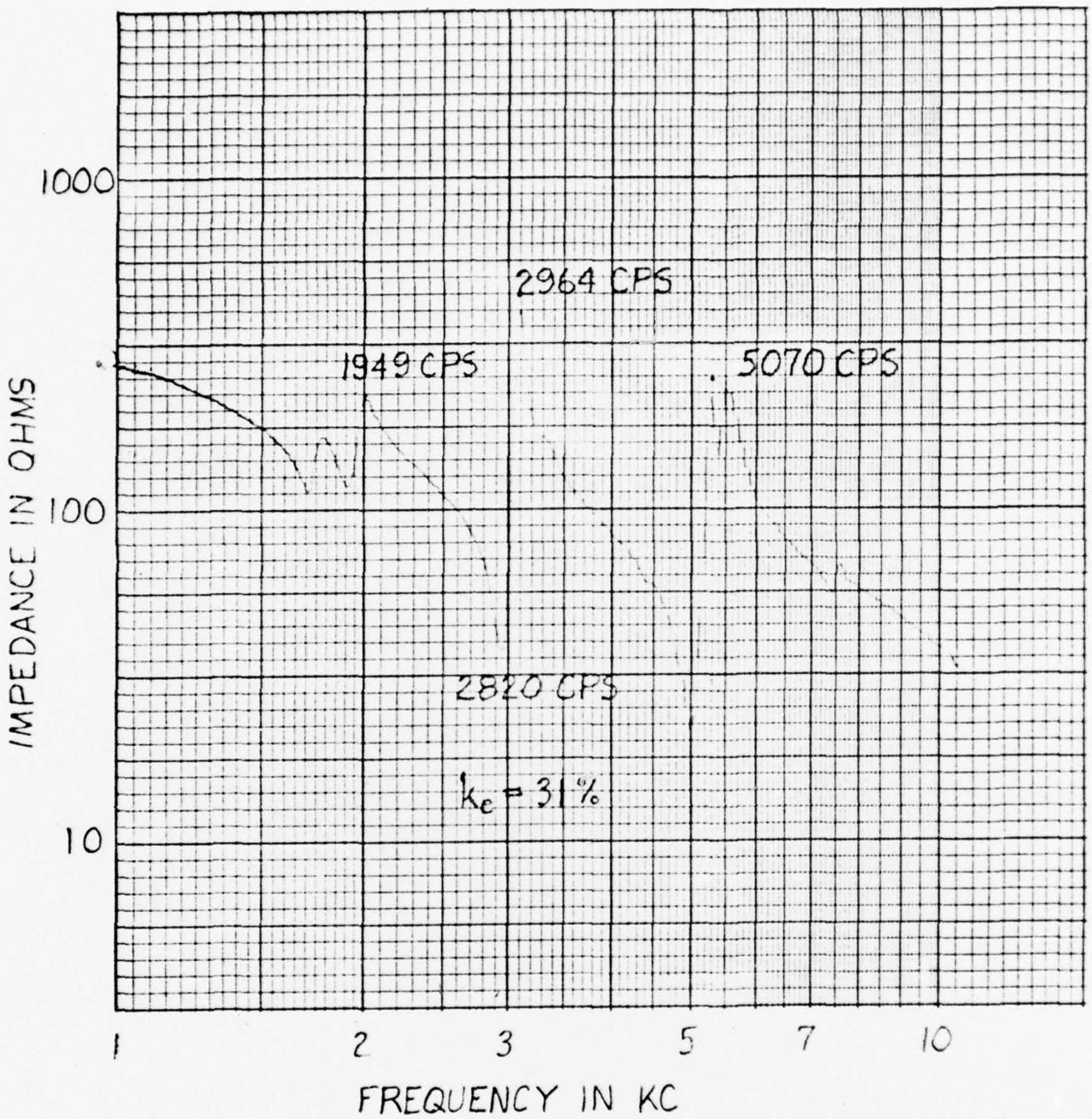

FIGURE 5. CONSTANT CURRENT FREQUENCY RESPONSE OF F2-2 IN AIR (OIL FILLED)

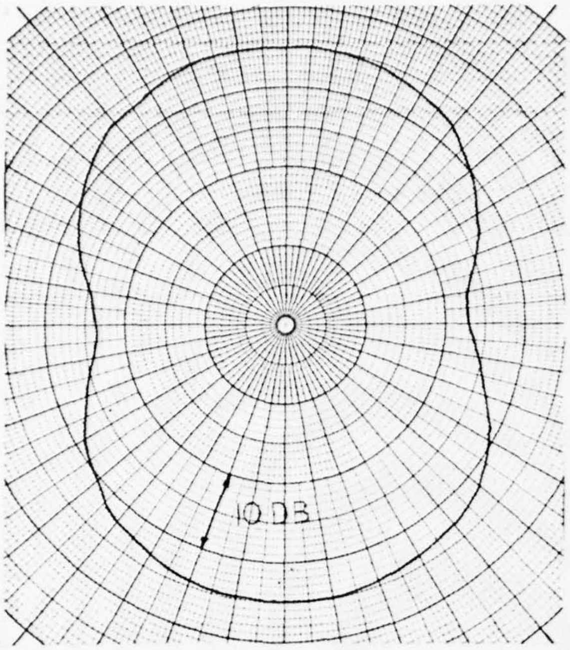

a. 1715 CPS

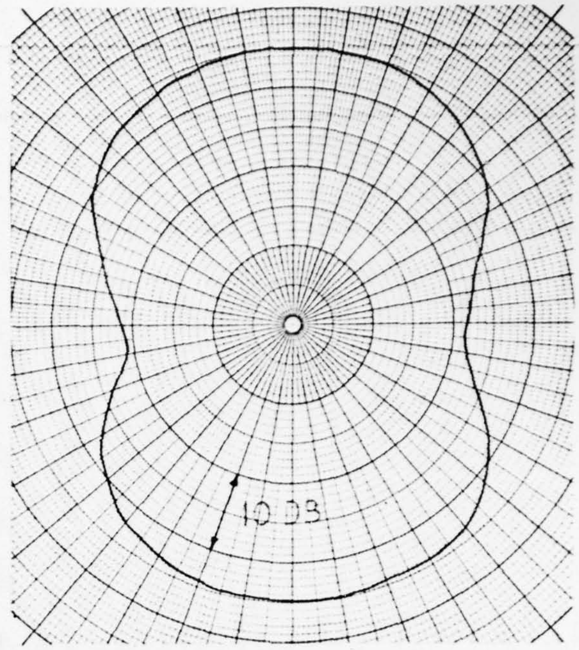

b. 2500 CPS

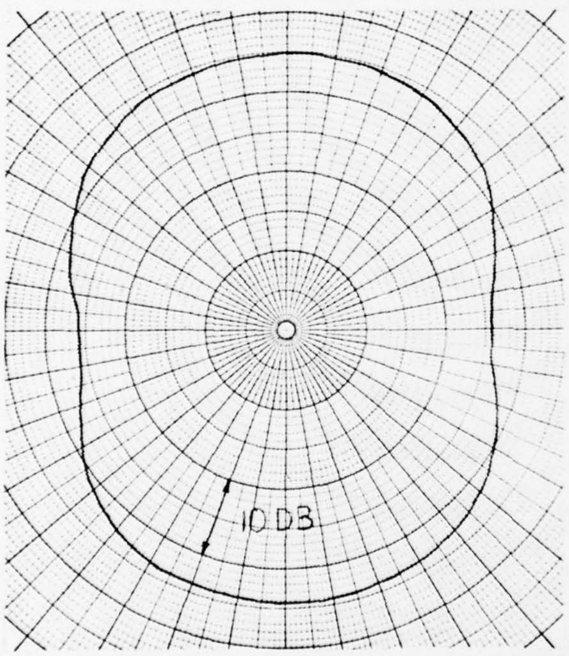

c. 2827 CPS

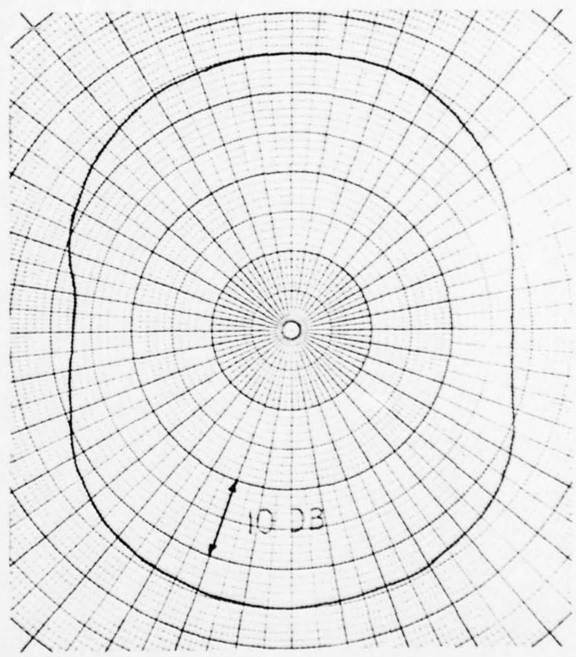

d. 3000 CPS

FIGURE 6. POLAR PATTERNS FOR F2-2 TRANSDUCER IN THE YZ PLANE

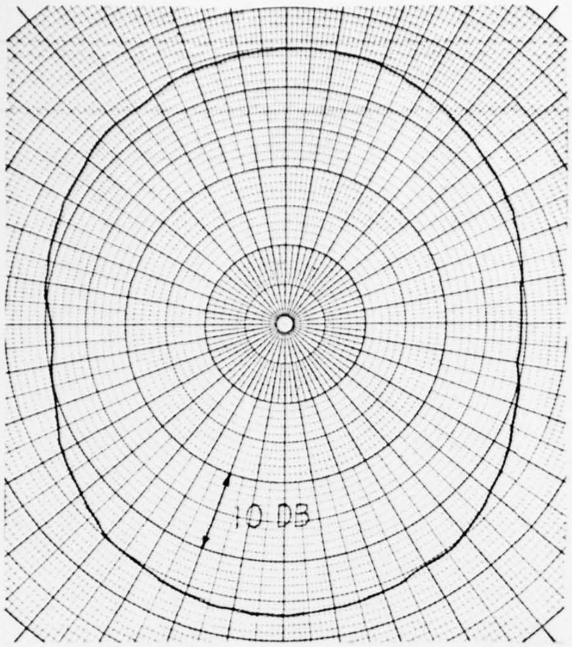

e. 3300 CPS

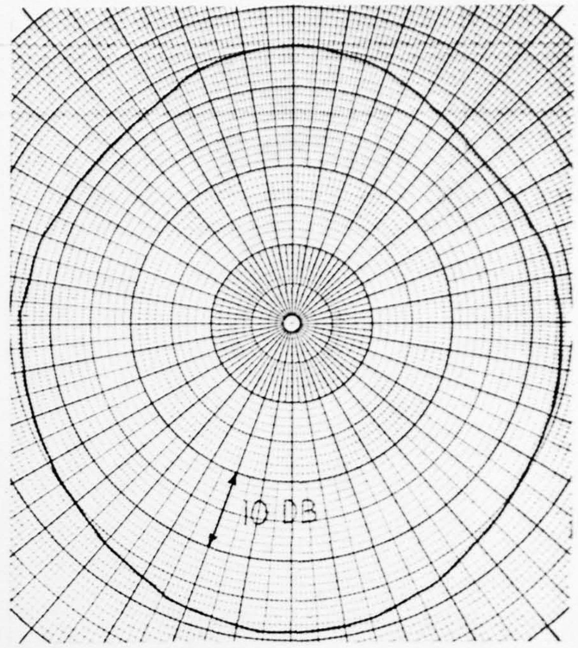

f. 3700 CPS

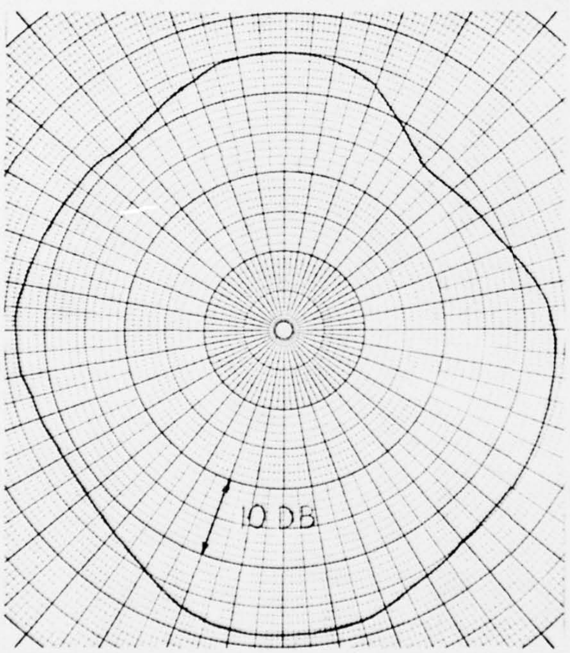

g. 4000 CPS

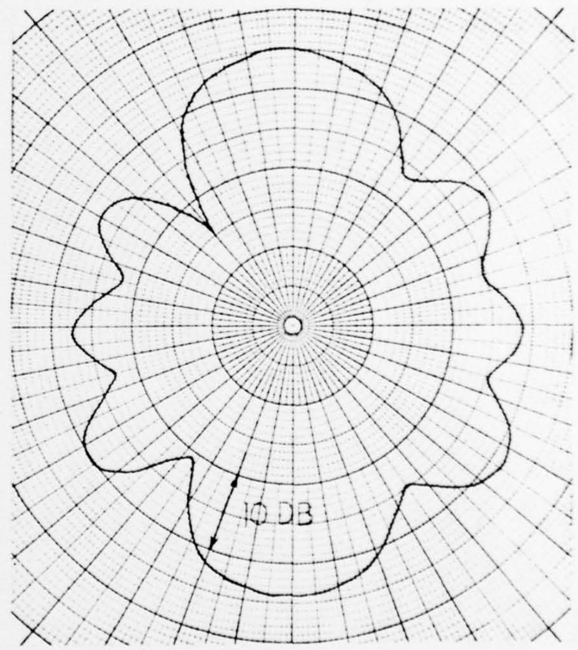

h. 4300 CPS

FIGURE 7. POLAR PATTERNS FOR F2-2 TRANSDUCER IN THE YZ PLANE

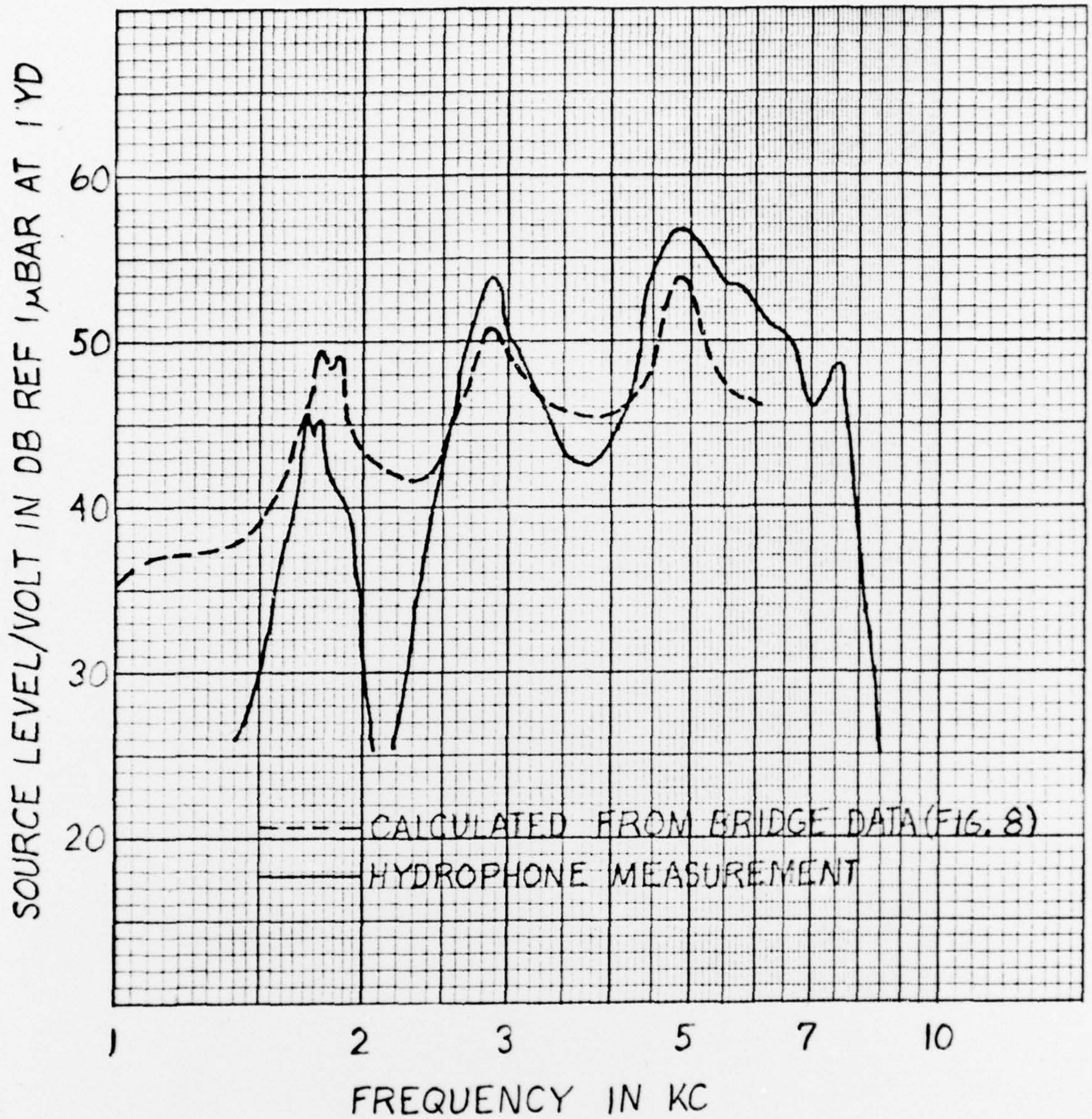

FIGURE 8. SOURCE LEVEL/VOLT FROM HYDROPHONE AND BRIDGE DATA FOR F2-2 TRANSDUCER

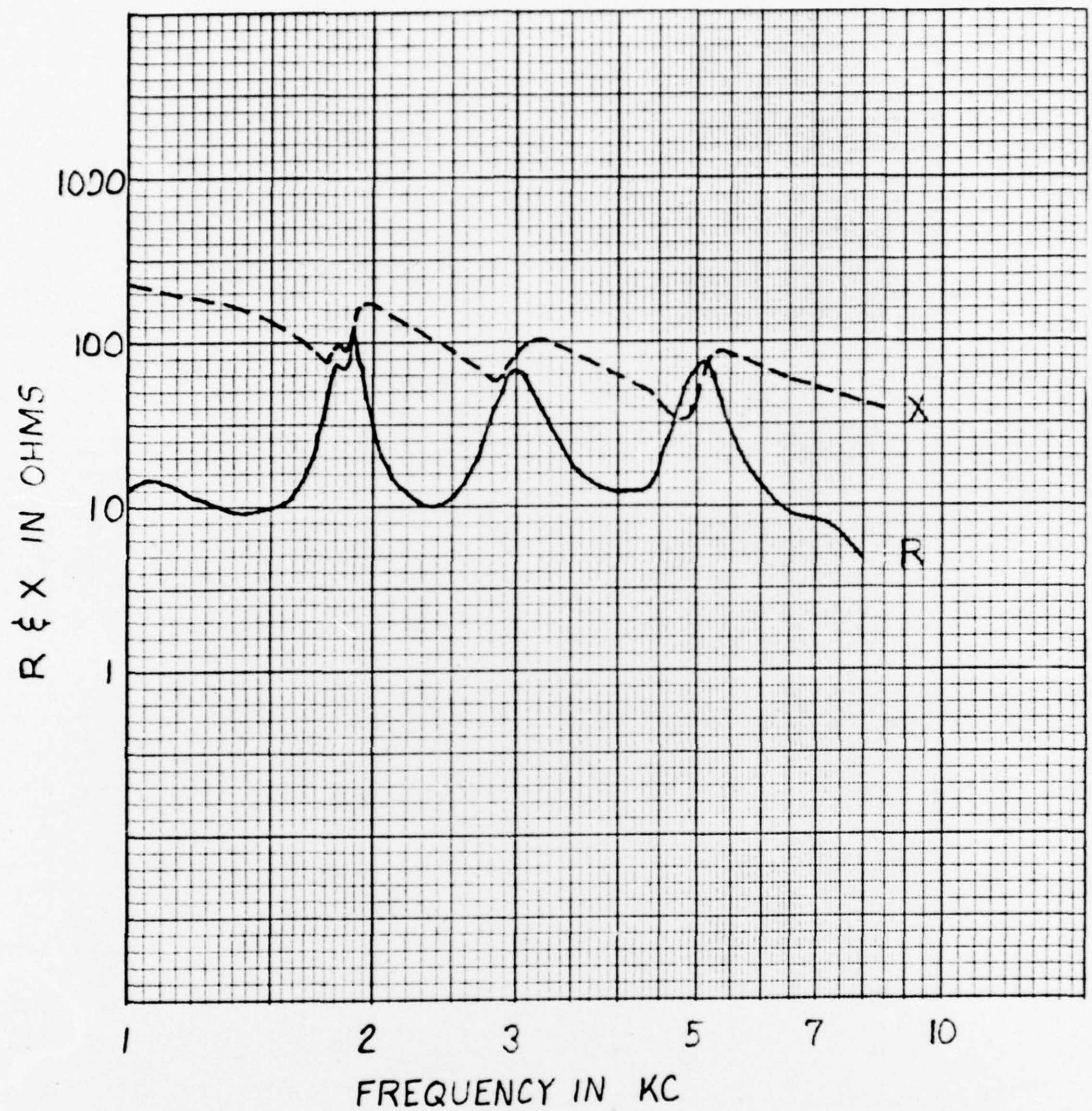

FIGURE 9. BRIDGE DATA OF R & X FOR F2-2 TRANSDUCER

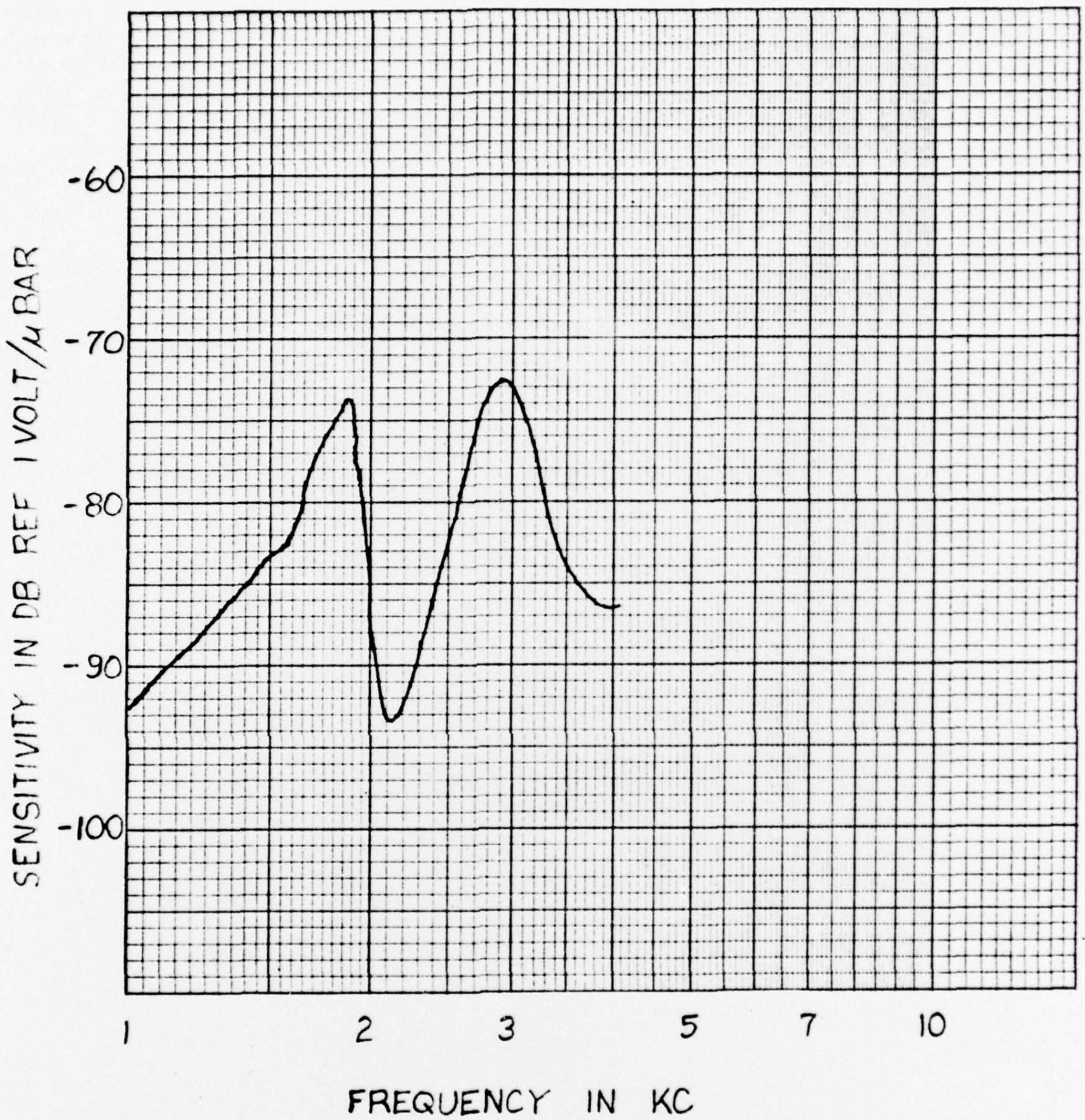

FIGURE 10. RECEIVING RESPONSE OF F2-2 TRANSDUCER

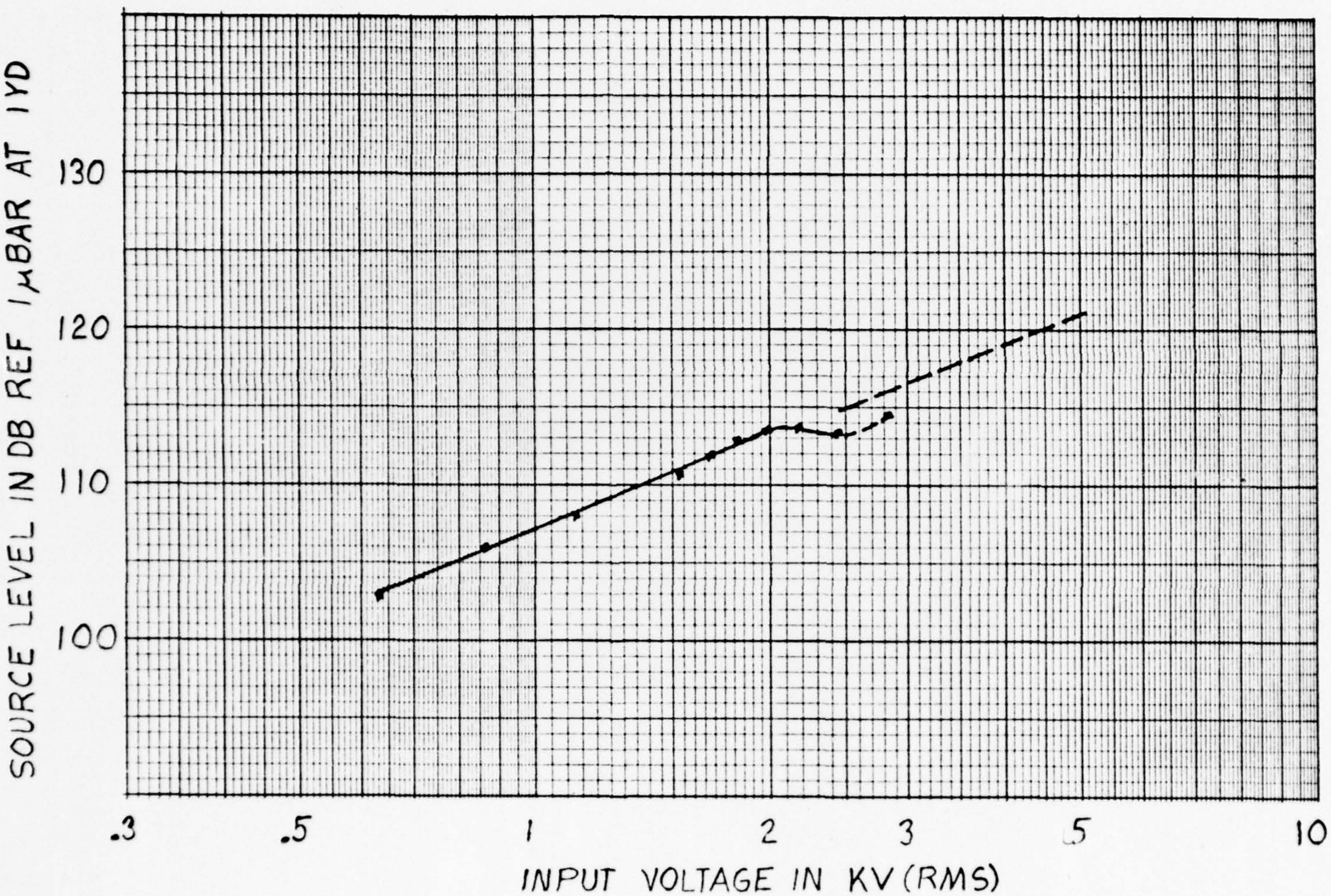

FIGURE 11. SOURCE LEVEL VS. INPUT VOLTAGE FOR F2-2

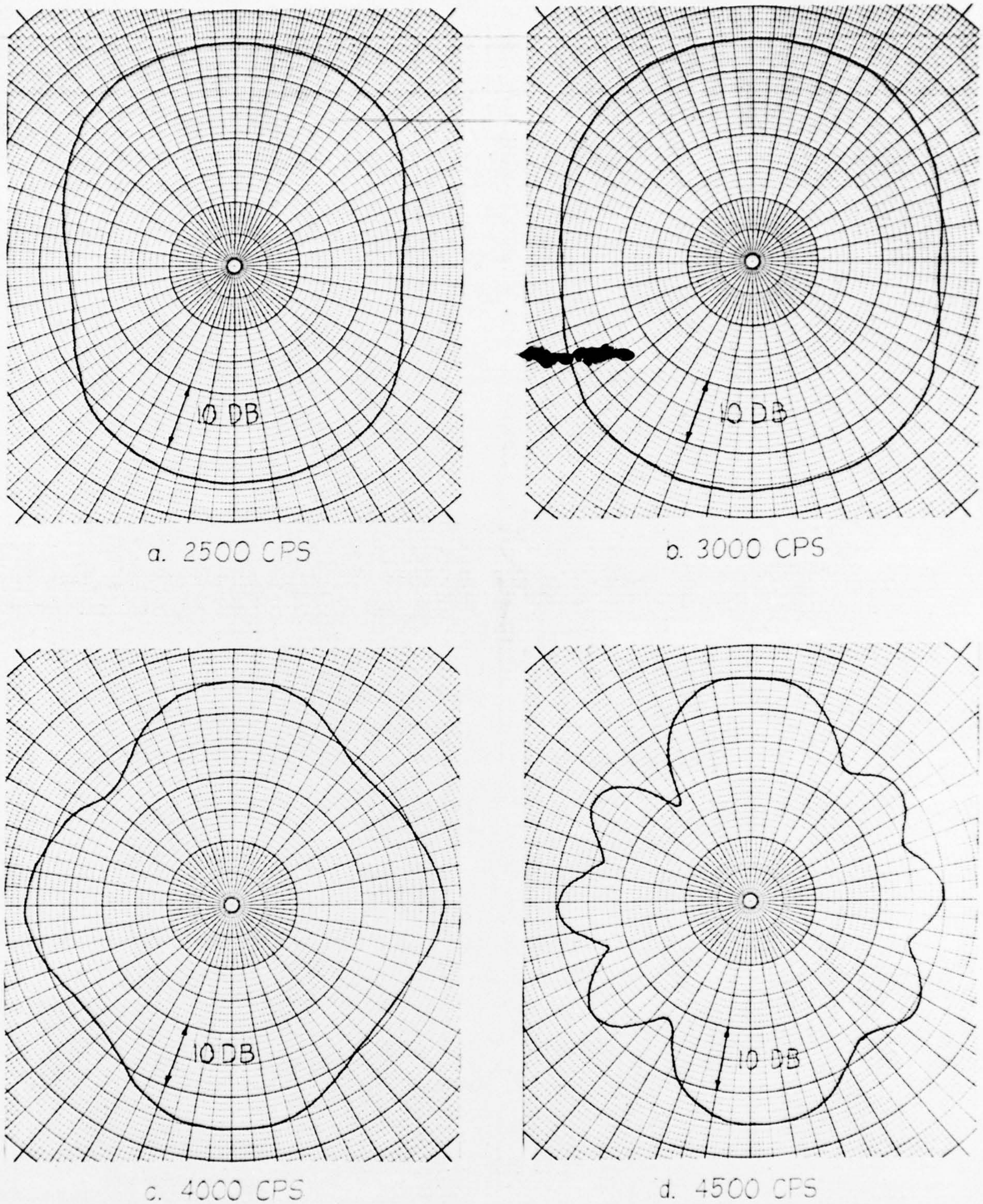

FIGURE 12. POLAR PATTERNS FOR F2-1 TRANSDUCER IN THE YZ PLANE

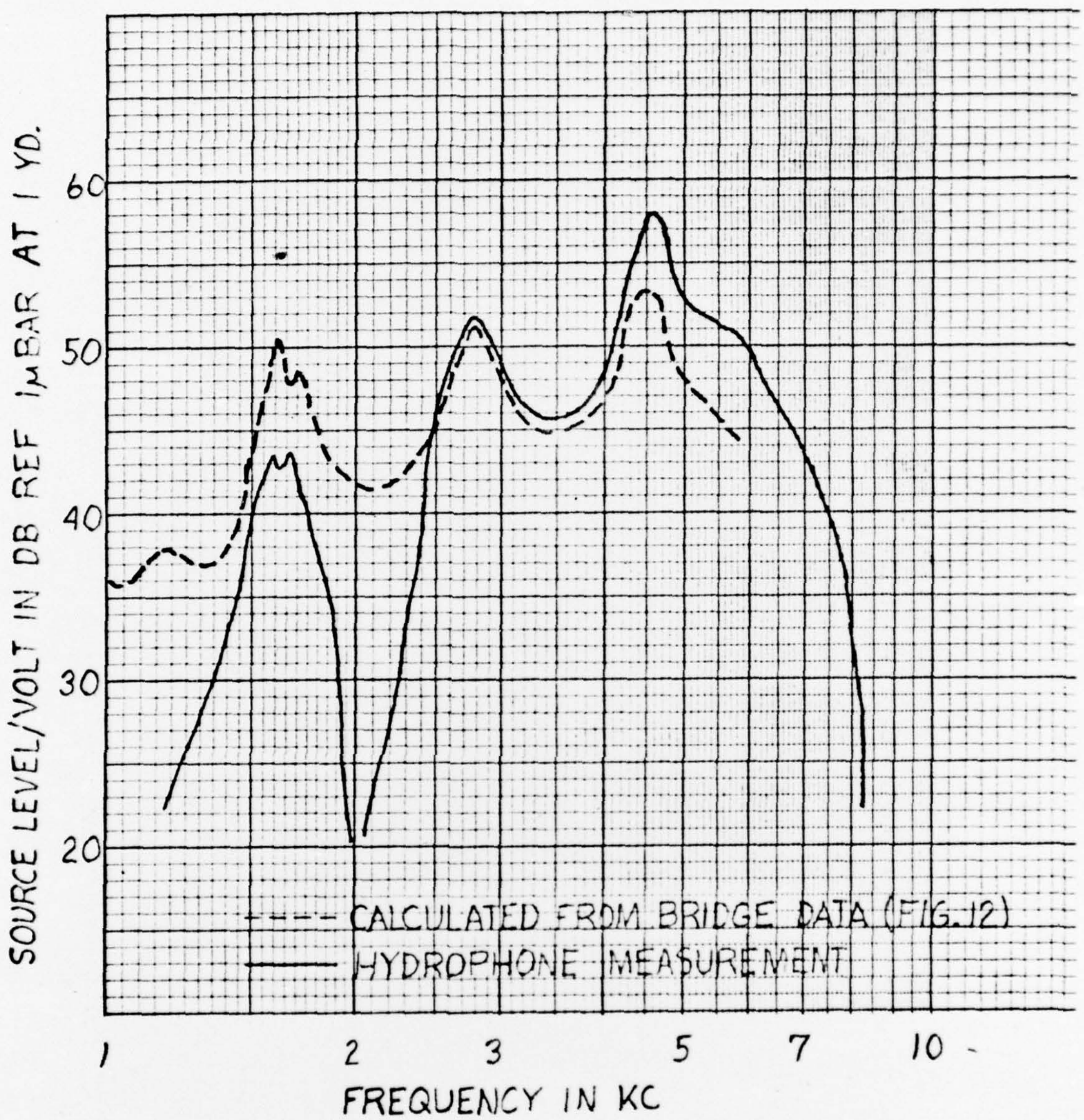

FIGURE 13. SOURCE LEVEL/VOLT FROM HYDROPHONE AND BRIDGE DATA FOR F2-1 TRANSDUCER

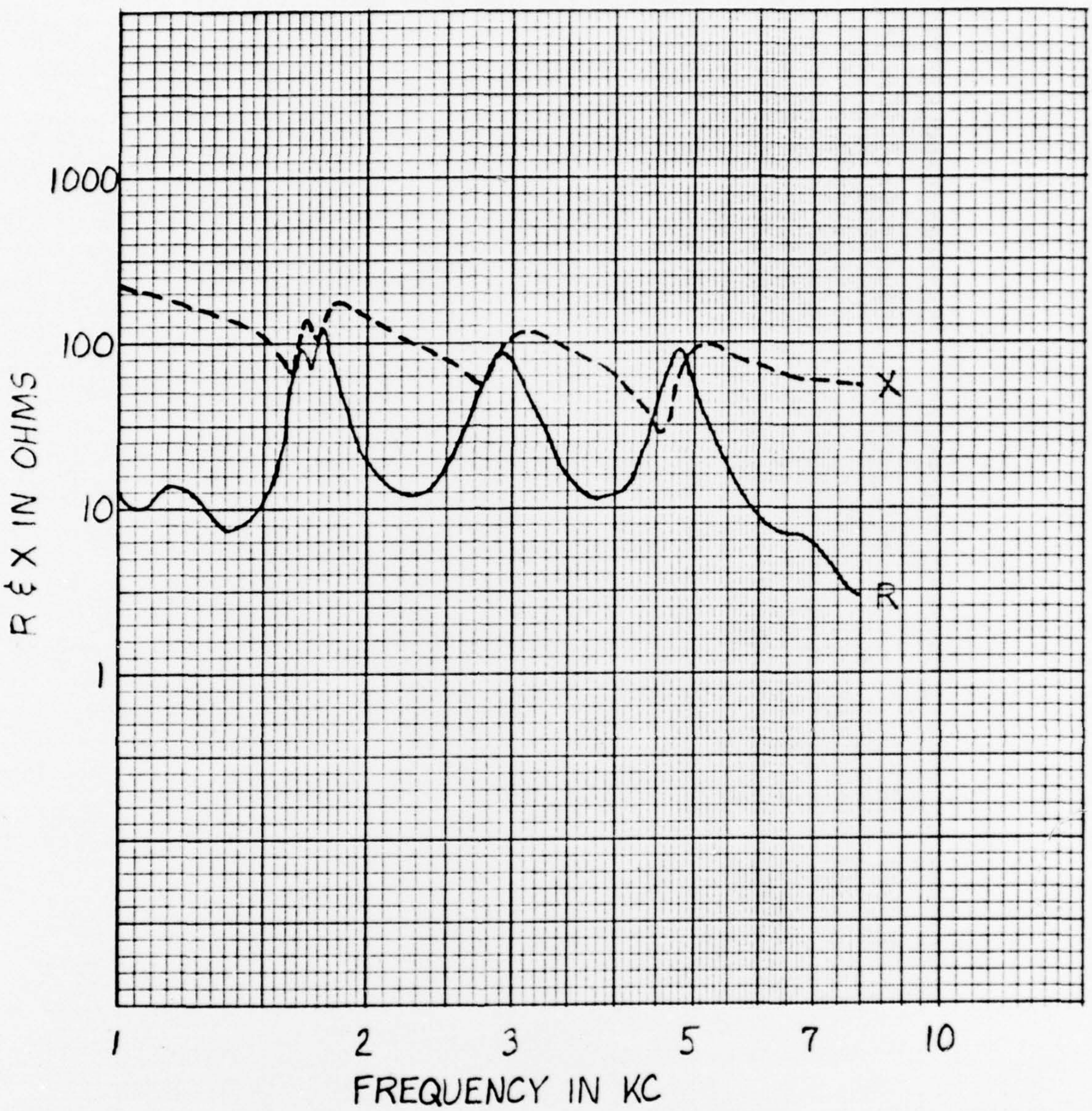

FIGURE 14. BRIDGE DATA OF R & X FOR F2-1 TRANSDUCER

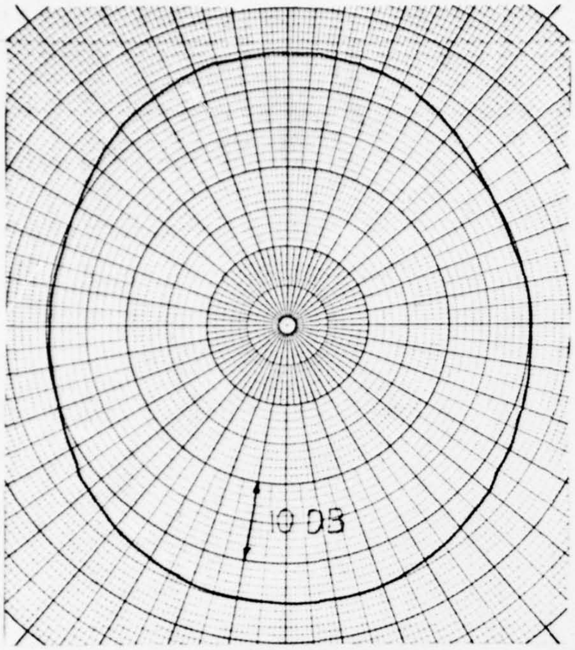

a. 1670 CPS

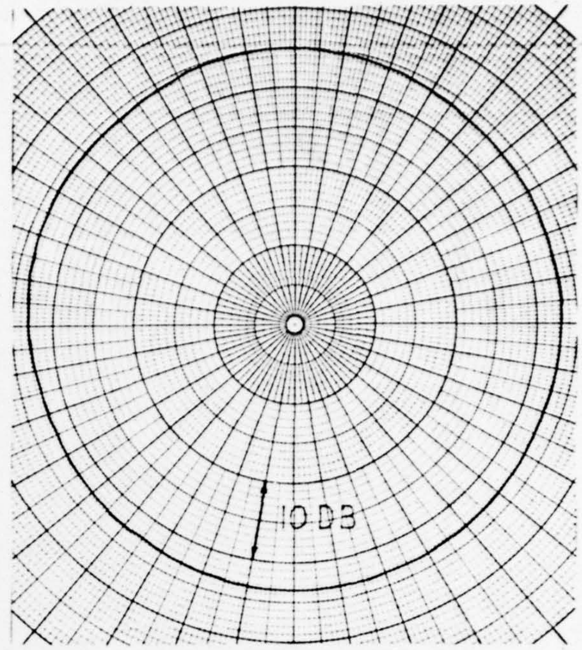

b. 2925 CPS

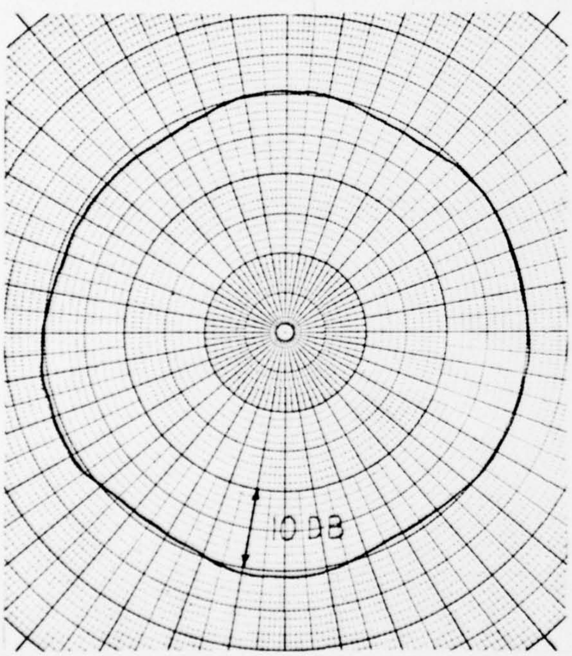

c. 4000 CPS

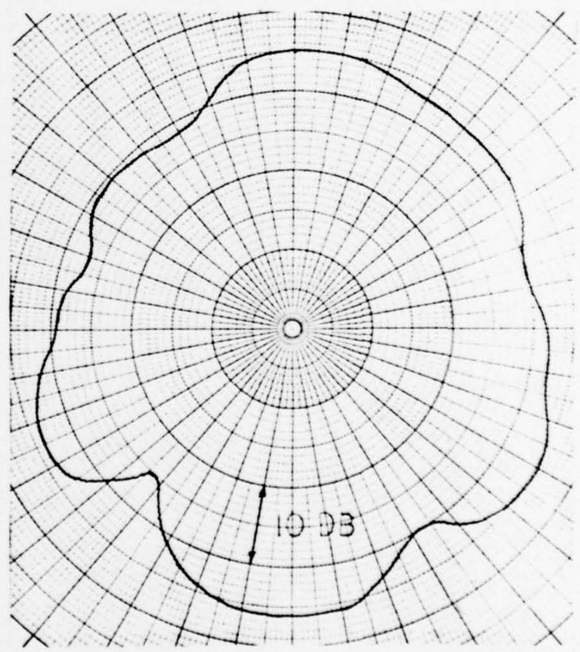

d. 5000 CPS

FIGURE 15. POLAR PATTERNS AT NAA-COLUMBUS FOR F2-2 TRANSDUCER IN THE YZ PLANE

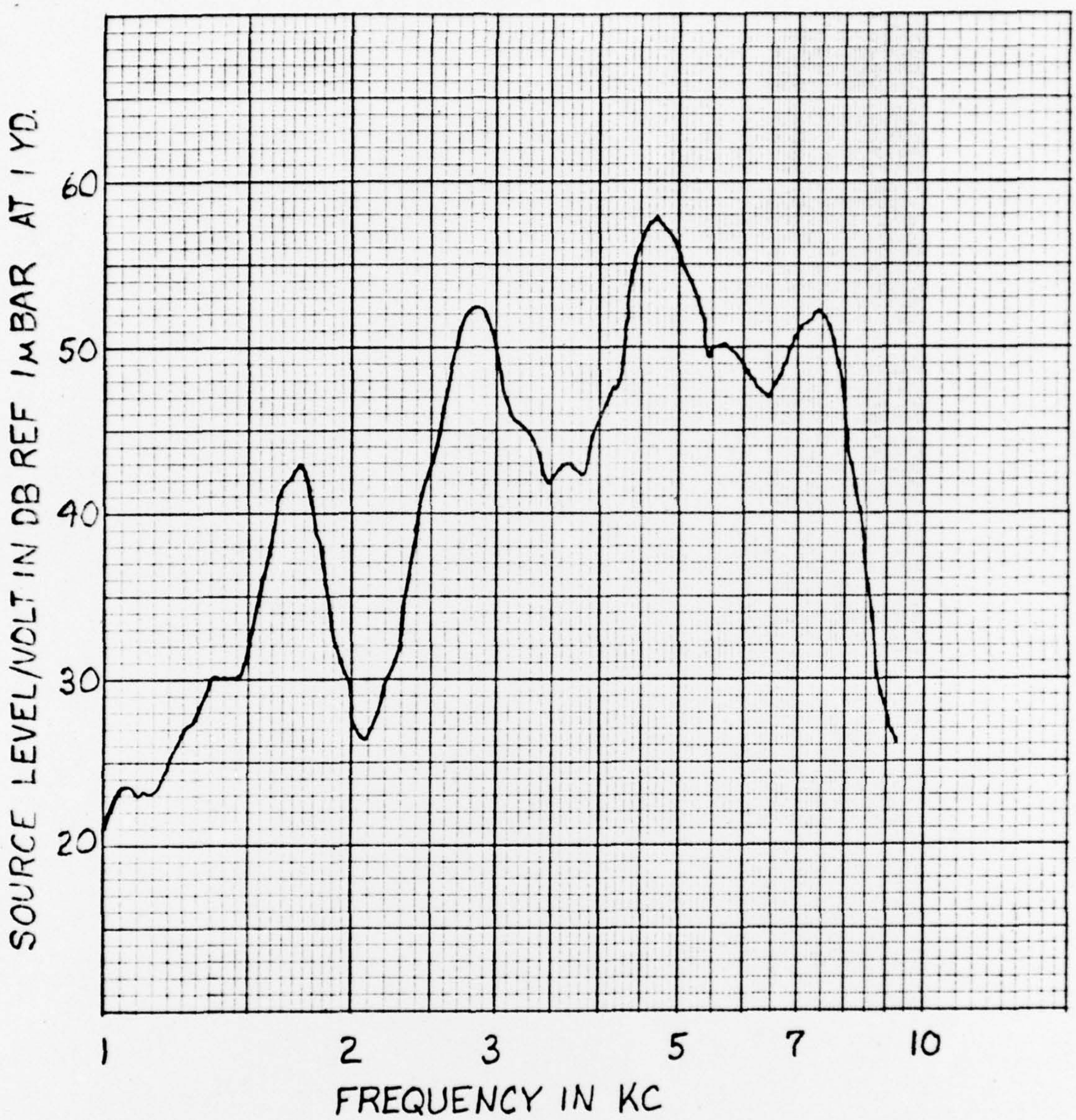

FIGURE 16. SOURCE LEVEL/VOLT FROM HYDROPHONE FOR F2-2 AT NAA-COLUMBUS

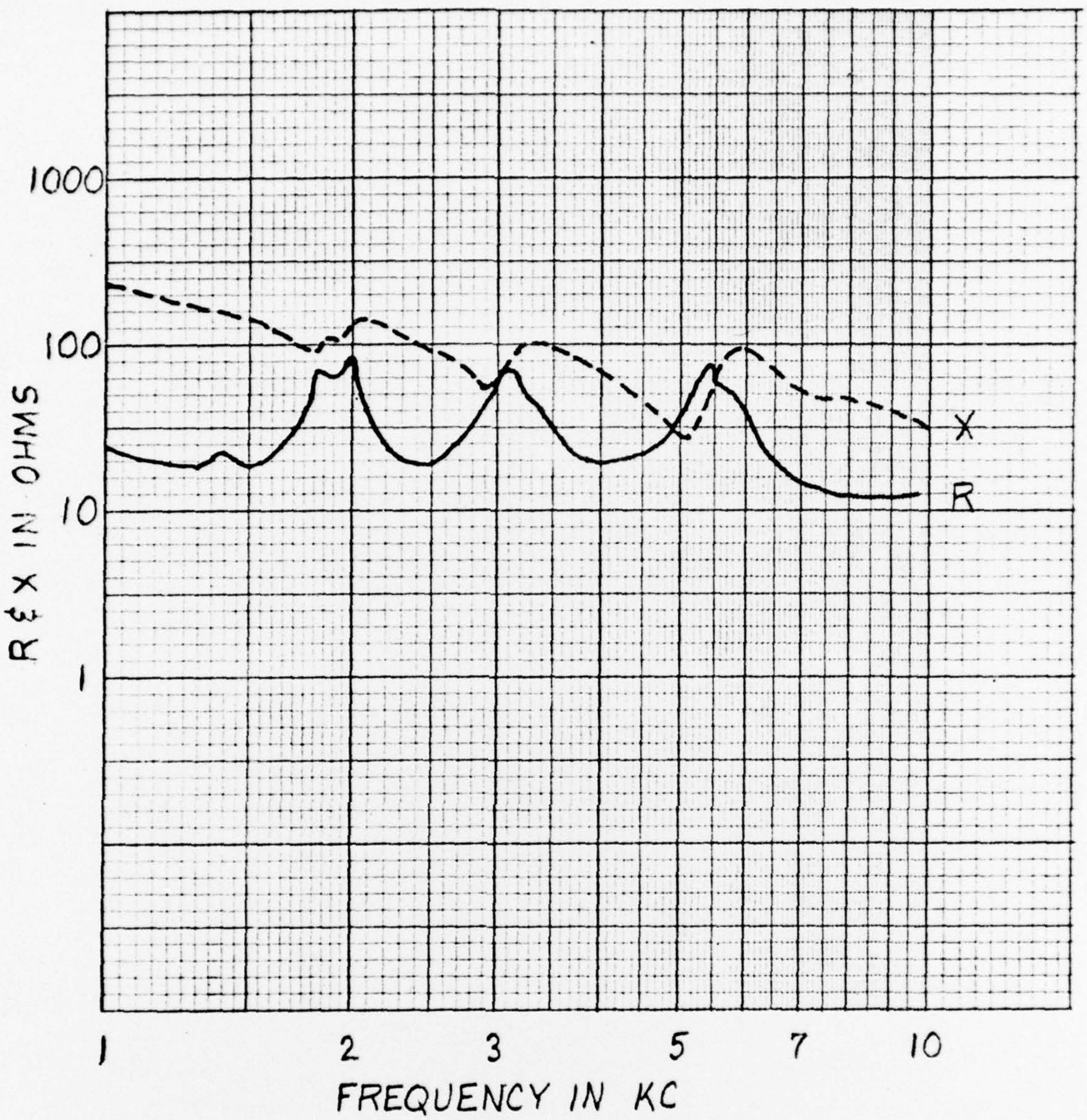

FIGURE 17. BRIDGE DATA OF R & X FOR F2-2 TRANSDUCER AT NAA-COLUMBUS

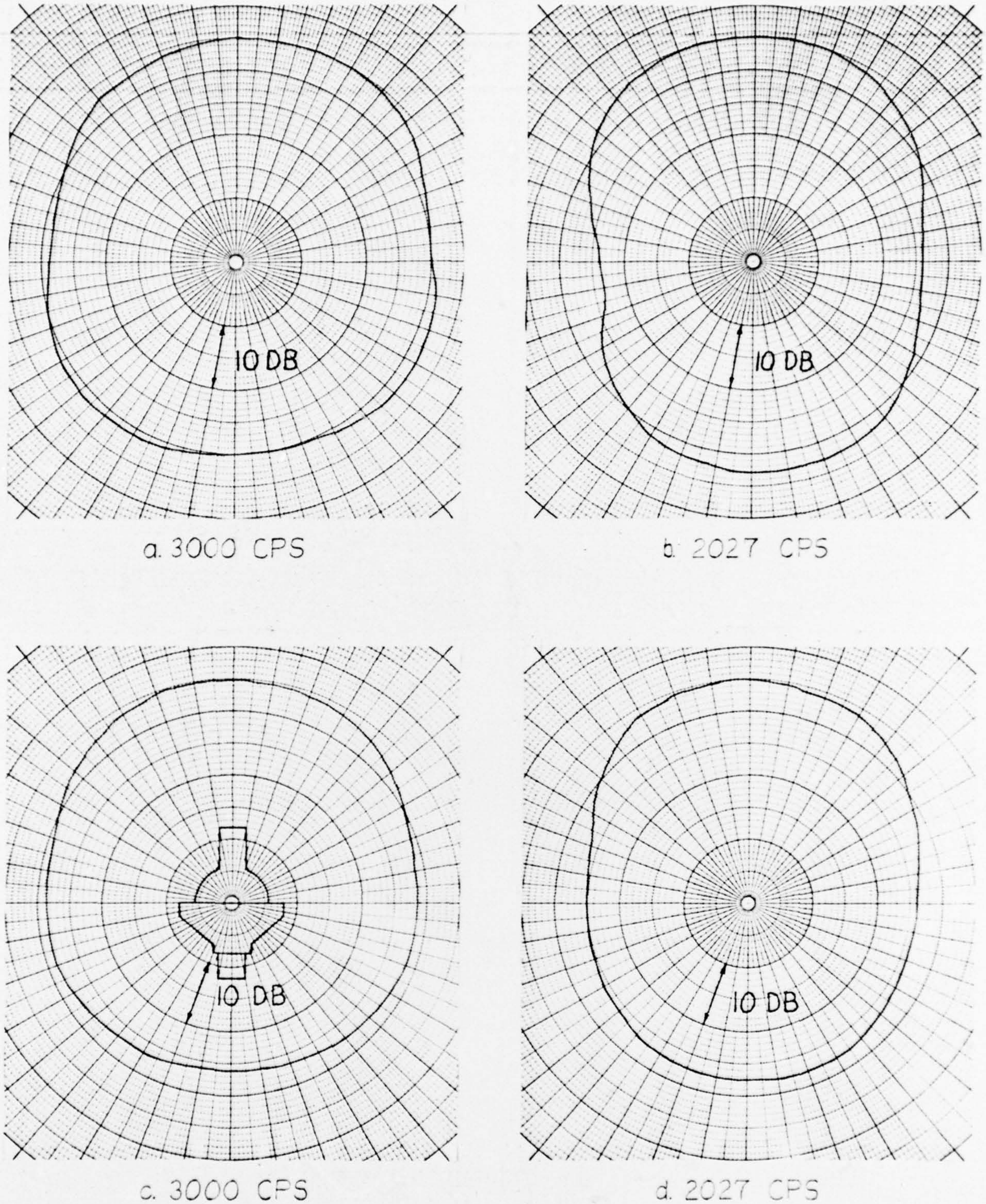

FIGURE 18. POLAR PATTERNS AT NAA-COLUMBUS FOR F2-1 WITH STEEL CONICAL REFLECTOR IN THE YZ PLANE. a AND b WITHOUT CELLTITE BACKING. c AND d WITH CELLTITE

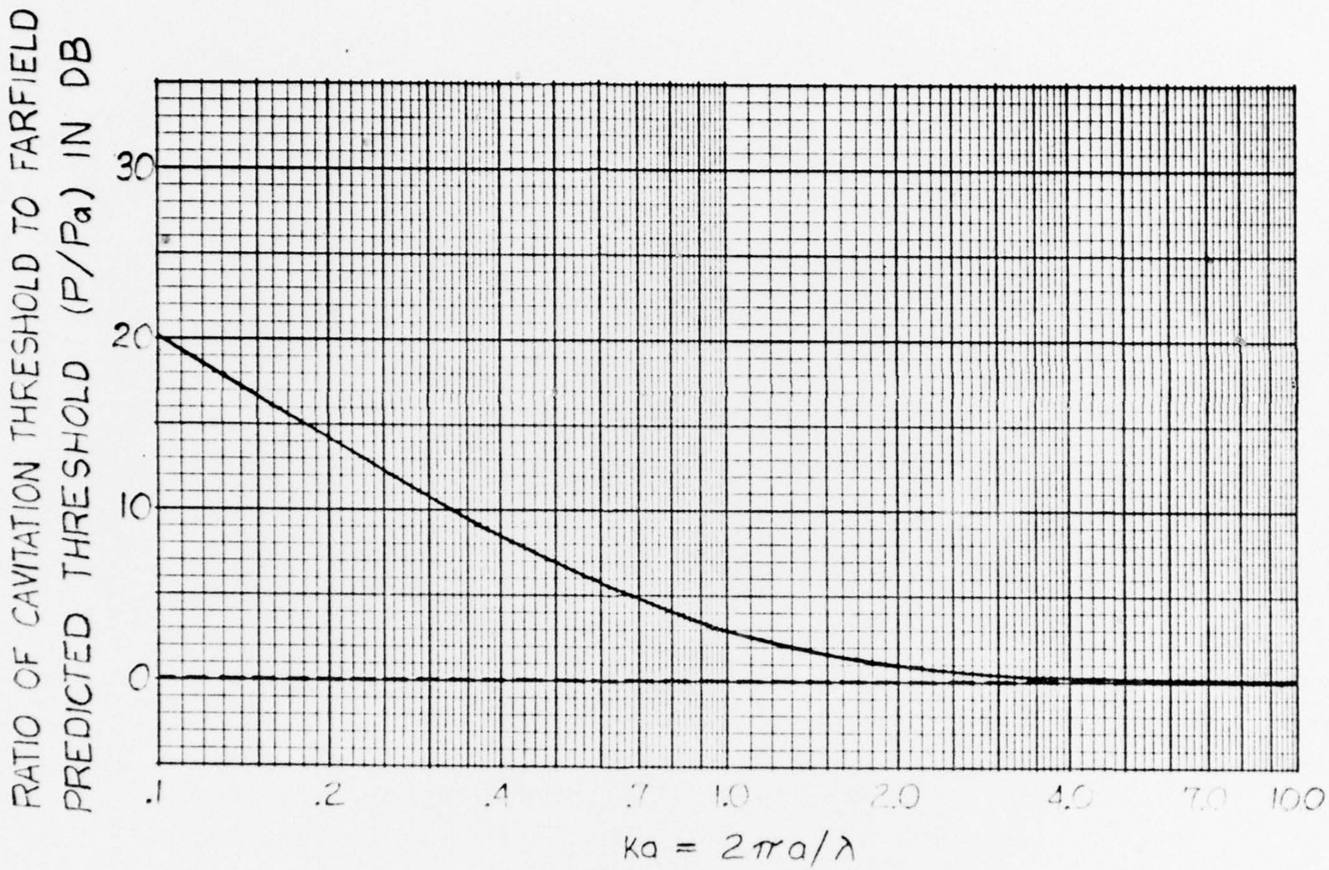

FIGURE 19. DEGRADATION OF CAVITATION LIMIT VS Ka